ADVANCED HEALTHCARE MATERIALS
www.advhealthmat.de

Rational Design of Glucose-Responsive Insulin Using Pharmacokinetic Modeling

*Naveed A. Bakh, Gili Bisker, Michael A. Lee, Xun Gong, and Michael S. Strano**

A glucose responsive insulin (GRI) is a therapeutic that modulates its potency, concentration, or dosing of insulin in relation to a patient's dynamic glucose concentration, thereby approximating aspects of a normally functioning pancreas. Current GRI design lacks a theoretical basis on which to base fundamental design parameters such as glucose reactivity, dissociation constant or potency, and in vivo efficacy. In this work, an approach to mathematically model the relevant parameter space for effective GRIs is induced, and design rules for linking GRI performance to therapeutic benefit are developed. Well-developed pharmacokinetic models of human glucose and insulin metabolism coupled to a kinetic model representation of a freely circulating GRI are used to determine the desired kinetic parameters and dosing for optimal glycemic control. The model examines a subcutaneous dose of GRI with kinetic parameters in an optimal range that results in successful glycemic control within prescribed constraints over a 24 h period. Additionally, it is demonstrated that the modeling approach can find GRI parameters that enable stable glucose levels that persist through a skipped meal. The results provide a framework for exploring the parameter space of GRIs, potentially without extensive, iterative in vivo animal testing.

1. Introduction

Diabetes mellitus (DM) is a family of diseases characterized by chronically high blood glucose levels (hyperglycemia) and impaired glucose metabolism.[1] Chronic hyperglycemia can lead to long-term organ damage resulting in blindness, renal failure, and increased risk of cardiovascular and peripheral vascular disease.[1] In the absence of effective treatment, extreme cases of hyperglycemia, called ketoacidosis, can result in coma or death.[1,2] However, insulin overdose can result in acute low blood glucose, or hypoglycemia, which can also be fatal.[3]

Insulin is a peptide hormone, produced by the β-cells of the pancreas, that is responsible for the regulation of glucose homeostasis in the body.[1] In diabetics there are complications with either the self-production or the efficacy of insulin. The majority of diabetic cases fall under two main types.[1,4] Type 1 diabetes results from the autoimmune destruction of the pancreatic β-cells, resulting in a complete lack of insulin production, and patients who depend on exogenous insulin for survival.[1] Type 2 diabetes results from abnormal insulin production and insulin resistance, and patients may require exogenous insulin for blood glucose control if diet and exercise are insufficient.[1,2] Strict glycemic control is necessary for the treatment of all forms of diabetes. This is accomplished primarily by adhering to a strict schedule of insulin administration along with lifestyle changes.[5] However, glycemic control is difficult due to the open loop nature of the problem (**Figure 1**a) and the large patient-to-patient variation in response to insulin treatment.[6] Additionally, physicians report that the majority of their patients do not maintain their insulin regiment properly.[7] Furthermore, tight blood glucose control is difficult to achieve due to concessions given to reduce hypoglycemia risk.[7] Technological developments have been made to attempt to close the loop so that insulin dosing is directly controlled by the patient's blood glucose levels. Continuous glucose monitoring (CGM) in conjunction with an insulin infusion pump has shown significant improvement over injection therapy in maintaining glycemic control, while minimizing the need for patient adherence and lowering hypoglycemia incidents.[8] However, CGM with insulin pumps are expensive and the implanted components both increase the risk of inflammation and require frequent replacement due to the body's immune response.[9,10]

A different strategy for achieving closed loop insulin administration, and a longstanding goal of DM treatment, comes from the expanding field of insulin delivery technologies that are responsive to the glucose concentration of their environment.[11] These glucose-responsive insulins (GRIs) have the ability to sense the local glucose concentration through various chemistries and subsequently trigger insulin release. The common features of all the GRIs include a glucose sensing mechanism and a trigger for insulin release, activation of potency, or biological accessibility. Each specific GRI has advantages and disadvantages ranging from biocompatibility to insulin release kinetics.[11] The end goal of such technologies is to develop a synthetic pancreas to control blood glucose levels.[12] The literature to date describes four distinct mechanistic schemes of GRI constructs. The majority of GRIs have been based on polymeric systems loaded with glucose oxidase (GOx). The GOx oxidizes glucose to form D-glucono δ-lactone,

N. A. Bakh, Dr. G. Bisker, M. A. Lee, Dr. X. Gong, Prof. M. S. Strano
Department of Chemical Engineering
Massachusetts Institute of Technology
77 Massachusetts Avenue, Cambridge, MA 02139, USA
E-mail: strano@mit.edu

DOI: 10.1002/adhm.201700601

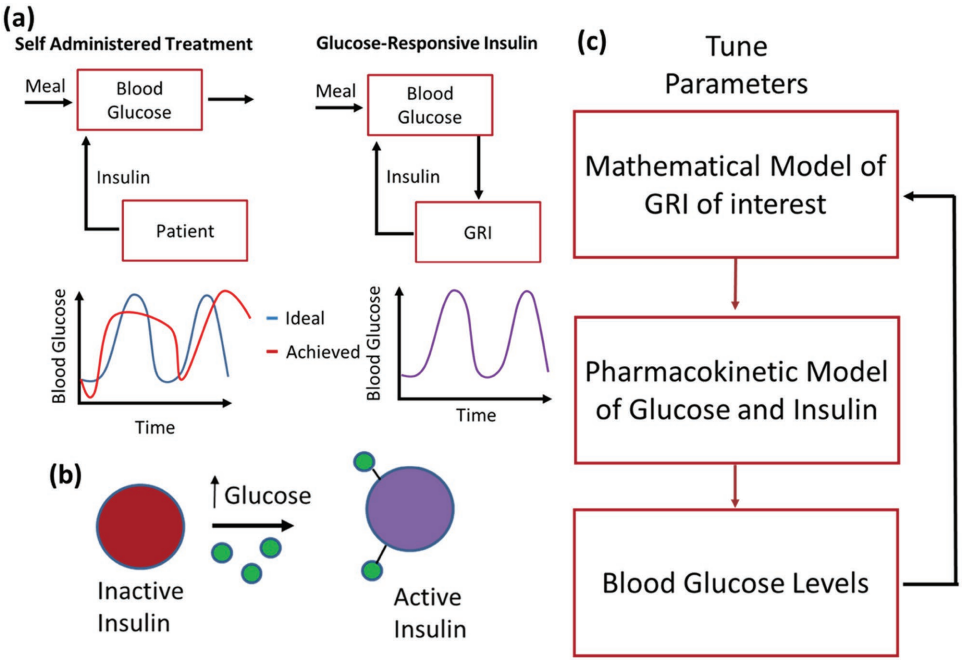

Figure 1. a) Illustrates the open loop problem of insulin self administration where the patient has difficulty controlling the amount of insulin to dose (blue curve is ideal blood glucose and red curve is achieved blood glucose), while a well developed GRI can accurately control blood glucose levels (shown by overlapping blue and red curves). b) Shows a schematic of the freely circulating GRI that activates upon binding with glucose. c) Shows the general approach taken for evaluating GRI parameters using a combination of a pharmacokinetic models with theoretical models of GRIs.

which then hydrolyzes to gluconic acid.[13] The gluconic acid lowers the pH, which triggers the release of insulin from the polymer. *Scheme I*—enzyme-based GRIs that rely on acid labile groups on the polymer, which erode under acidic conditions and release entrapped insulin.[14] *Scheme II*—uses GOx and ionic polymer swelling to control insulin release. Polycationic polymers, such as a polymer containing amine groups, become charged at low pH leading to electrostatic repulsion that causes polymer swelling thus triggering insulin release.[15,16] Others have developed GRIs taking advantage of the shrinking properties of polyanionic membranes to form collapsible pores to control insulin release.[17] Much work has been done to refine these GOx based GRIs, such the coencapsulation of catalase with GOx to regenerate the oxygen needed for glucose oxidation and these formulations have demonstrated good glycemic control in mice.[18] *Scheme III*—polymers, which are made with glucose binding moieties such as lectins or phenylboronic acids (PBA), that use competitive binding to control swelling.[19,20] The glucose binding moieties are incorporated into the hydrogel and used to crosslink polymers containing saccharide-like groups. In the presence of glucose these crosslinks are disrupted due to competitive binding resulting in polymer swelling and subsequent insulin release. *Scheme IV*—chemically modified, freely circulating insulin molecule that is sensitive to glucose. Recently, insulin modified with an aliphatic chain to bind albumin for increased circulation time and PBA to bind glucose has been shown to achieve glycemic control in mice over 12 h with a single large dose (Figure 1b).[21] In this work we combine the mathematical representation of a Scheme IV GRI with a human physiological model to determine the parameters that maximize glycemic control. We consider GRIs based on Scheme IV due to constituting the most recent direction for this research, as well as their mathematical simplicity. Our future work will extend our approach to the other GRI schemes, which are also being actively pursued.[18,22]

There have been limited efforts to mathematically model the operations of a GRI within the human body, and to date, they have not linked efficacy to material or molecular design parameters.[23–25] Instead, modeling of Scheme I and II GRIs have focused on the enzyme reactions themselves or the insulin diffusivity inside various polymer formulations.[23–25] The central contribution of our work is linking GRI design parameters to therapeutic efficacy. We assert that the large number of GRIs being proposed and demonstrated require a standardized framework to evaluate their limits and efficacy as an insulin therapeutic. A common experimental approach in GRI development is to empirically test candidate constructs in vivo within an animal model to evaluate the therapeutic effectiveness,[18,21,22] in what amounts to a costly and time consuming development process. A mathematical modeling framework for GRI design could potentially predict GRIs performance before testing in animal models, and narrow the parameter space for desired synthesis, or inform clinicians on dosing of newly synthesized GRIs with known parameters.

The GRI is also an important emerging model for other future drugs designed to modulate their potency, concentration or release kinetics in response to some therapeutic endpoint measured within the human body. Our work then is motivated by a growing need for a framework that provides chemists and biologists guidelines for choosing design parameters such as

analyte reactivity, enzyme loadings, crosslinking density, molecular release profiles, and other important parameters for drug efficacy. In the case of GRI, the explicit target is the optimal glycemic control in patients. To develop these guidelines we combine a mathematical model of a GRI with a pharmacokinetic model of glucose-insulin metabolism to directly couple the GRI parameters with efficacy (Figure 1c). This approach is a flexible one, where any glucose-insulin metabolic model can be combined with any mathematical formulation of the various GRI schemes described above. This mathematical formulation can allow ex vivo tests to rule out unfeasible GRIs and minimize animal studies. Additionally, scaling drugs from animal models to the clinic could benefit by comparing experimental and theoretical results of therapies in animals to human pharmacokinetic models and data to elucidate the differences that may arise in efficacy. In this work we use a compartment model based on the work of Sorensen,[26] which has previously been used by Parker et al. to develop model based control algorithms for closed loop blood glucose control.[27–29] Additionally, our group has modified the Sorensen model to divide the peripheral compartment into muscular and adipose tissue.[30] In this work, we will further modify the model with the goal of exploring theoretical Scheme IV GRIs.[31] As a demonstration of the flexibility and the importance of model selection, the glucose insulin model developed by Dalla Man[32–35] is used to model the same theoretical Scheme IV GRI in the Supplementary Information.

2. Model Formulation

2.1. Model Compartment Descriptions—Sorensen

We use a physiological model to track the concentrations of glucose, glucagon, and insulin in the major compartments of the body in order to predict the effect of insulin released from a GRI. We note that the freely circulating GRI of Scheme IV reported by Chou can be described by the following equation, where glucose can act as a switch to activate the freely circulating insulin modeled by the following reversible chemical reaction

$$G + D \underset{k_{-1}}{\overset{k_1}{\rightleftarrows}} I \qquad K_{eq} = \frac{k_1}{k_{-1}} \tag{1}$$

where G is glucose, D is dormant insulin (representing inactivate GRI), I is active (or native) insulin, k_1 and k_{-1} are the forward and reverse rate constants, and K_{eq} is the equilibrium constant for the reaction. The metabolic pathways of these molecules were modeled according to Sorensen[26] and Bisker et al.[30]

The Sorensen[26] approach is a pharmacokinetic model which divides the body into well mixed compartments where the blood volume, containing glucose and insulin, circulates through the capillary volumes and solutes are free to diffuse between the capillary volume and the interstitial volumes. The equations for a generic solute in a compartment taking into account the GRI reaction are as follows

$$V_{kc}^{s}\frac{dC_{kc}}{dt} = Q_k(C_H - C_{kc}) - \frac{V_{ki}^{s}}{T_k^{s}}(C_{kc} - C_{ki}) - r_{suc} + r_{spc} + V_{kc}^{I}\nu_s r_{GRI} \tag{2}$$

$$V_{ki}^{s}\frac{dC_{ki}}{dt} = \frac{V_{ki}^{s}}{T_k^{s}}(C_{kc} - C_{ki}) - r_{sui} + r_{spi} + V_{ki}^{I}\nu_s r_{GRI} \tag{3}$$

where k is the subscript referring to the compartment, c or i are the subscripts referring to the capillary or interstitial volume, respectively, s is a superscript or a subscript which denotes the type of solute, V is the volume of the compartment, C is the concentration of the solute in the compartment (G, D, I, or glucagon), Q is the arterial flowrate for that compartment, T is the transcapillary mass transfer time, and r_u and r_p are the uptake or production rates (in mass per time) of the solute in that compartment, respectively. The reaction rate for the GRI equation is r_{GRI}, which is set to zero if we are modeling native insulin. Additionally, r_{GRI} is assumed to only occur in the volume accessible by insulin, and has units of mass per volume per time, thus it is converted to mass per time with V^I in each compartment. The stoichiometric coefficient is defined as ν_s, where $\nu_G = -1$, $\nu_D = -1$, and $\nu_I = 1$. The GRI reaction rate, based on the concentrations of solutes, in each compartment is defined below

$$r_{GRI} = k_1[G][D] - k_{-1}[I] \tag{4}$$

We track 4 solutes: glucose, glucagon, insulin, and dormant insulin. The compartments for dormant insulin were assumed to be the same as those for regular insulin. If the transcapillary mass transfer is rapid enough, the capillary and interstitial volumes can be modeled as a single well mixed compartment. As was done previously, the heart and lungs, liver, gut, and kidneys were modeled as a single compartment in all the glucose, insulin, and dormant insulin systems. The periphery was divided into two compartments as shown by Equations (2) and (3) in both the glucose and insulin subsystem. The brain was divided into two compartments for the glucose system, whereas for the insulin subsystem it was treated as a single compartment due to insulin's inability to diffuse into cerebrospinal fluid.[26] **Figure 2** shows a schematic of the compartment model along with our modifications. **Table 1** defines the variables used in the model. The Sorensen parameters are defined for a 70 kg healthy man and all the equations used in development of the model can be found in the supplemental information. Additionally, the parameters and concentrations are based on the accessible water volume for each solute, because glucose and insulin cannot diffuse throughout the entirety of whole blood. Therefore the glucose and insulin volumes and flowrates were decreased by 16% and 40% from the whole blood volume, respectively. To properly capture clinical values, the vascular glucose concentrations of the model must be decreased by 16% to reflect whole blood glucose levels, and by 7.5% to reflect blood plasma levels.[26]

The Sorensen model has a number of limitations, such as the inability to describe patient variability due to the basis of the parameters being a healthy 70 kg male.[26] Not only will this result in difficulty in using the model for different sized

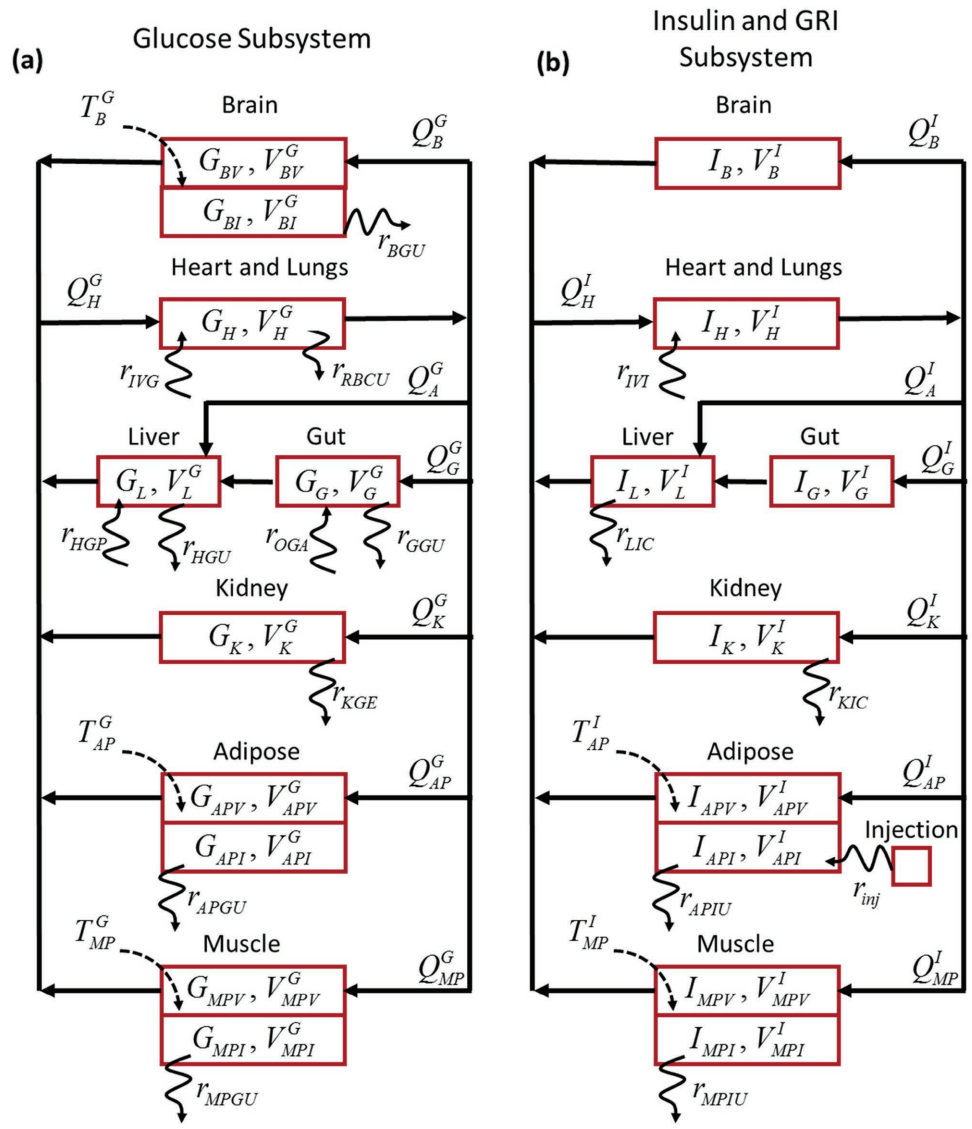

Figure 2. a) Schematic of the compartments for the glucose system. b) Schematic of the insulin and dormant insulin (if applicable) systems. Blood circulates from the heart and lungs through the vasculature of the brain, liver, gut, kidney, adipose, and muscular tissues. In the glucose system, the brain, adipose, and muscular tissues are separated into two compartments due to slow transcapillary mass transfer into the interstitial space. In the insulin system, the brain is a single compartment due to insulins inability to penetrate the interstitial space. A subcutaneous injection compartment is shown transferring insulin or dormant insulin to the interstitial adipose tissue.

patients, but the model also has difficulty capturing metabolic abnormalities which are sometimes present in diseased patients.[26] Additionally, the model parameters do not describe rodents, where most of the GRIs are tested experimentally, making it difficult to predict current experimental data. However, our goal with this work is to show that the approach of using a physiological model in combination with mathematical constructs of GRIs to optimize parameters for glycemic control is a viable one. To simulate a diabetic patient with the Sorensen model, the rate of pancreatic insulin release, r_{PIR}, is set to zero, resulting in an otherwise metabolically normal Type 1 diabetic model[26] with tight blood glucose control.[26] More work needs to be done in the future on the development of physiological compartment models that can accurately account for differences in metabolism of diabetic patients. However, for the purposes of this work, we will focus on the metabolically normal Type 1 diabetic model described above.

2.2. Subcutaneous Injection Compartment

Injection of insulin is usually performed subcutaneously into the adipose tissue. Our modified model has accounted for an adipose compartment; however, there are many factors affecting insulin absorption such as blood flow rates, insulin type, concentration, and dose.[36,37] Models have been developed that assume the existence of an injection depot with the same size as the injection volume. The insulin or GRI injected in the

Table 1. A list of the variables, subscripts, and superscripts used in the model.

Compartment variables		Injection compartment	
G	Glucose concentration	I_{dm}	Dimer concentration
I	Insulin concentration	I_{hex}	Hexamer concentration
D	Dormant insulin concentration	x_{dm}	Dimer mass
Q	Blood flow rate	x_{hex}	Hexamer mass
r	Reaction rate	V_{inj}	Injection volume
T	Transcapillary diffusion time	D_{inj}	Diffusivity of insulin
t	Time	k_{abs}	Absorption rate constant
k_1, k_{-1}	GRI rate constants	k_2, k_{-2}	Dimer/hexamer rate constants
F	Fractional clearance		**Metabolic rate**
Compartment subscript		GRI	Glucose responsive insulin
B	Brain	BGU	Brain glucose uptake
H	Heart and lungs	RBCU	Red blood cell glucose uptake
G	Gut	GGU	Gut glucose utilization
L	Liver	HGU	Hepatic glucose uptake
K	Kidney	KGE	Kidney glucose excretion
P	Periphery	APGU	Adipose peripheral glucose uptake
AP	Adipose periphery	MPGU	Muscle peripheral glucose uptake
MP	Muscular periphery	IVG	Intravenous glucose infusion
A	Hepatic artery	OGA	Gut oral glucose absorption
Subcompartment subscript		HGP	Hepatic glucose producton
I	Interstitial	LIC	Liver insulin clearance
V	Vascular	KIC	Kidney insulin clearance
Superscript		APIC	Adipose periphery insulin clearance
G	Glucose	MPIC	Muscle peripheral insulin clearance
I	Insulin (and GRI)	IVI	Intravenous insulin infusion

depot is assumed to take either hexameric or dimeric forms based on the following equilibrium equation[38–40]

$$3I_{dm} \underset{k_{-2}}{\overset{k_2}{\rightleftarrows}} I_{hex}$$
$$I_{hex} = K_H I_{dm}^3 \tag{5}$$

where I_{dm} is the concentration of dimeric insulin or GRI, and I_{hex} is the concentration of hexameric insulin or GRI, k_2 and k_{-2} are the forward and reverse rate constants, and K_H is the equilibrium constant. The initial masses of hexamer and dimer are calculated with the above equilibrium ratio based on a 100 U mL^{-1} injection concentration. Both forms of insulin are allowed to diffuse, thus increasing the size of the injection depot and decreasing the insulin concentration. Only the dimeric insulin can be absorbed into the body.[38,41] Due to computational complexity, we adopted the approach of Wong, who modeled the diffusive loss and hexamer conversion as simple kinetic rate constants, and fit these rate constants against experimental plasma insulin profiles from a variety of patients treated with various insulin analogs.[39,40] The initial insulin was injected at equilibrium through an instantaneous bolus as described above and the mass balances for the depot were as follows[39,40]

$$\frac{dx_{dm}}{dt} = k_{-2}x_{hex} - k_{abs}x_{dm} - k_d x_{dm}$$
$$\frac{dx_{hex}}{dt} = -k_{-2}x_{hex} - k_d x_{hex} \tag{6}$$

where x_{dm} and x_{hex} are the mass of dimeric and hexameric insulin (or GRI), respectively, k_{abs} is the absorption rate into the body, and k_d is the rate constant for diffusion. For a specific mass of injected insulin and injection volume, the equilibrium mass of dimers and hexamers are calculated beforehand and used as the initial conditions for above differential equations.[39,40] The diffusion effect is described by the following rate constant[39,40]

$$k_d = \frac{3D_{inj}}{r_{inj}^2}$$
$$r_{inj} = \left(\frac{3V_{inj}}{4\pi}\right)^{1/3} \tag{7}$$

where D_{inj} is the diffusivity of hexameric and dimeric insulin (taken to be the same), and r_{inj} is the radius of the injection volume which is V_{inj}. In our modified Sorensen model the injection depot is adjacent to the adipose peripheral interstitial compartment, and the dimeric insulin diffuses into that space. Hence, the updated adipose tissue equation for native insulin injection is as follows

$$V_{API}\frac{dI_{API}}{dt} = \frac{V_{APV}^I}{T_{AP}^I}(I_{APV} - I_{API}) - r_{APIC} + k_{abs}x_{dm} \tag{8}$$

If a GRI is being modeled, then the insulin is injected into the depot as dormant insulin, and we assumed the injection kinetics of dormant insulin behaved in the same manner as native insulin due to sensitivity analysis performed on k_{abs} shown in the Supplementary Information. The updated adipose tissue equations for GRI injection, instead of native insulin, is as follows

$$V_{API}^I\frac{dD_{API}}{dt} = \frac{V_{API}^I}{T_{AP}^I}(D_{APV} - D_{API}) - V_{API}^I(k_1 D_{API}G_{API} - k_{-1}I_{API}) + k_{abs}x_{dm} \tag{9}$$

2.3. Establishing Physiological Constraints

Next, we introduce a mathematical criteria to evaluate the efficacy of the theoretical GRI in question by establishing upper and lower limits for acceptable plasma glucose levels and quantifying the time periods in which our GRI maintains these levels throughout the evaluation period. These criteria or mathematical constraints can be directly adapted from clinical recommendations or desired outcomes. For example, according

to the American Diabetes Association (ADA), diabetes can be diagnosed based on either the glycated hemoglobin (A1C) criteria, which measures the attachment of glucose to hemoglobin, or the plasma glucose criteria.[42] Conveniently, since our model directly calculates plasma glucose levels, we can adopt the plasma glucose criteria of the ADA to use as an upper limit. The ADA states that 2 h after a 75 g oral glucose tolerance test diabetic patients will exhibit plasma glucose levels greater than 200 mg dL^{-1}, while prediabetic patients maintain plasma glucose levels between 140 and 200 mg dL^{-1}.[42] In this work, we have selected the stricter upper limit of 140 mg dL^{-1} as an acceptable plasma glucose level 2 h after each meal. The lower limit is defined as the plasma glucose level before the onset of hypoglycemia, whose threshold can vary from patient to patient. Some patients with poorly controlled diabetes can suffer hypoglycemic symptoms at higher glucose levels compared to the general population; however, despite these variations between patients, the ADA recommends that plasma glucose levels should not fall below ≈72 mg dL^{-1}.[3] In summary, the two-bound criteria we use for GRI performance evaluation is as follows:

1) Upper limit—140 mg dL^{-1} 2 h after each meal and initial insulin (or GRI) administration.
2) Lower limit—72 mg dL^{-1} for all time points.

These limits can be updated and adjusted as needed for specific patient needs, or to incorporate the results of new clinical observations.

2.4. Calculating Optimal GRI Design

To evaluate any theoretical GRI our model, we can initialize the model with the GRI at $t = 0$ and track the plasma glucose levels over 24 h while consuming three meals consisting of 75 g of glucose eaten at $t = 420$ min, $t = 720$ min, and $t = 1080$ min. The oral glucose absorption rate was adapted from Lehmann and Deutsch to and applied to the Sorensen model in our previous work,[26,30,43] which is further described in the supplemental information. In short, the glucose absorption rate increases linearly for some time, plateaus, and subsequently decreases until all of the glucose is absorbed. To evaluate if the GRI can maintain plasma glucose levels throughout the day, within the previously established limits, we calculate the following criteria

$$Z_{\text{hi}} = \int_{t_i+120}^{t_{i+1}} \max\left\{G_{\text{plasma}} - G_{\text{upper}}, 0\right\} \mathrm{d}t$$
$$Z_{\text{low}} = \int_{0}^{t_{\text{total}}} \max\left\{G_{\text{lower}} - G_{\text{plasma}}, 0\right\} \mathrm{d}t \quad (10)$$

where Z_{hi} and Z_{low} are integrals to evaluate blood glucose excursions from the criteria defined above for hyperglycemia and hypoglycemia, respectively. t_i is the time in minutes when a given meal i is consumed or the time when the initial insulin bolus is given. As stated in the criteria above, Z_{hi} is evaluated 2 h after the consumption of a meal up until the following meal or the end of the time period. Z_{low} is evaluated over the total time period, t_{total}, which is 24 h in this study. G_{plasma} is the plasma glucose concentration, G_{upper} is the upper limit to plasma glucose defined above, and G_{lower} is the lower limit to plasma glucose defined above. This results in five positive Z values, one value for Z_{low} and four values for Z_{hi}: $Z_{\text{hi,inject}}$, $Z_{\text{hi,meal1}}$, $Z_{\text{hi,meal2}}$, and $Z_{\text{hi,meal3}}$ evaluated post GRI addition ($120 < t < 420$), post first meal ($540 < t < 720$), second meal ($840 < t < 1080$), and third meal ($1200 < t < 1440$), respectively. The total deviation from healthy levels can be described by Z_{total} as shown below

$$Z_{\text{total}} = Z_{\text{low}} + Z_{\text{hi,inject}} + Z_{\text{hi,meal1}} + Z_{\text{hi,meal2}} + Z_{\text{hi,meal3}} \quad (11)$$

A high value of Z_{total} represents poor GRI efficacy since the plasma glucose concentration remained outside of critical values for a significant amount of time. In this work, the hyperglycemia and hypoglycemia excursions are given the same weight; however, Z_{hi} and Z_{low} could be adjusted to reflect a difference in risks associated with the above diabetic criteria.

3. Results and Discussion

3.1. Subcutaneous Insulin Dynamics

Levels of glucose, insulin, and glucagon are shown in **Figure 3** for a metabolically normal Type I diabetic patient following a

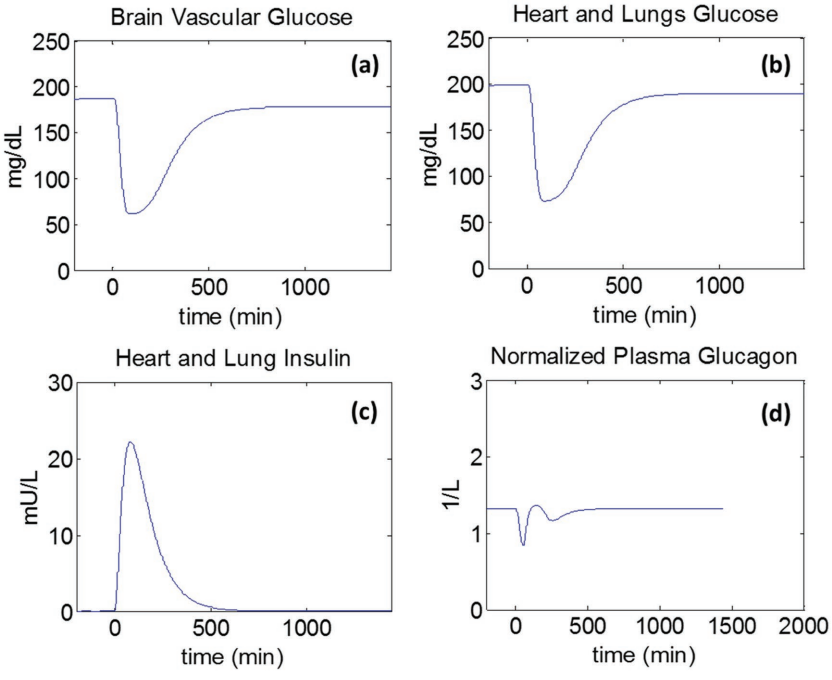

Figure 3. The dynamics of a 10 U subcutaneous injection of native insulin at $t = 0$ for the metabolically normal type 1 diabetic model showing the concentrations of glucose, insulin, and glucagon in select compartments. a) Brain vascular glucose, b) heart and lung glucose, c) heart and lungs insulin, and d) normalized plasma glucagon.

10 U subcutaneous injection of native (non-GRI) insulin at $t = 0$. The GRI reaction is set to zero in this simulation so that the insulin cannot convert to a dormant version. The dormant insulin compartments are removed from the set of differential equations. The arterial insulin rises to 22 mU L^{-1} at time $t = 78$ min, which is consistent with previous observations.[39,40] It can also be seen from the model that after the insulin peaks, the glucose in the heart and lung compartment increases back to the fasting diabetic steady state value of 200 mg dL^{-1}, which corresponds to a steady state plasma glucose of 185 mg dL^{-1} (92.5% of the heart and lung glucose concentration).

3.2. GRI Dynamics

The GRI type chosen in this work, the freely circulating GRI, can be described by two parameters—the forward rate constant k_1, and the equilibrium constant K_{eq}. For this study k_1 was varied between 10^{-4} and 10^4 M^{-1} min^{-1} and K_{eq} was varied between 10^{-2} and 10^6 M^{-1}. By changing these two parameters the effectiveness of the GRI (defined as its ability to maintain the blood glucose levels between the criteria described above) can be quantified by Z_{total}. **Figure 4** shows the dynamics and evaluation of blood glucose excursions for a 3 U kg^{-1} subcutaneous injection of GRIs with varying parameters for three meals of 75 g. Figure 4a presents a contour map of Z_{total} values as a function of the two critical GRI design variables, k_1 and K_{eq}. There is a clearly observable parameter space (blue) that minimizes Z_{total}, indicating optimal potency of the GRI. This suggests that with the proper formulation, an optimal GRI exists such that an individual can maintain blood glucose levels throughout the day after a three meal regiment without the need for additional injections of insulin. This is a desired feature of such a GRI. Figure 4b–d shows the resulting dynamics for blood glucose, blood active insulin, and blood dormant insulin for the GRI with the parameter values of $k_1 = 0.07$ M^{-1} min^{-1} and $K_{eq} = 0.33$ M^{-1} (the point denoted by the white dot in Figure 4a). It can be seen that, with these parameters, the blood glucose is above the critical hypoglycemia value (denoted by the lower red line) at all time-points and below the hyperglycemia cutoff (denoted by the upper red line) during the four periods that Z_{hi} was evaluated (regions denoted by the green background).

The individual contour plots for hypoglycemia excursions and hyperglycemia excursions after initial injection and the three meals are shown in the supplemental information. The Z_{hi} values for hyperglycemia excursions increase as the concentration of dormant GRI in the system decreases, suggesting

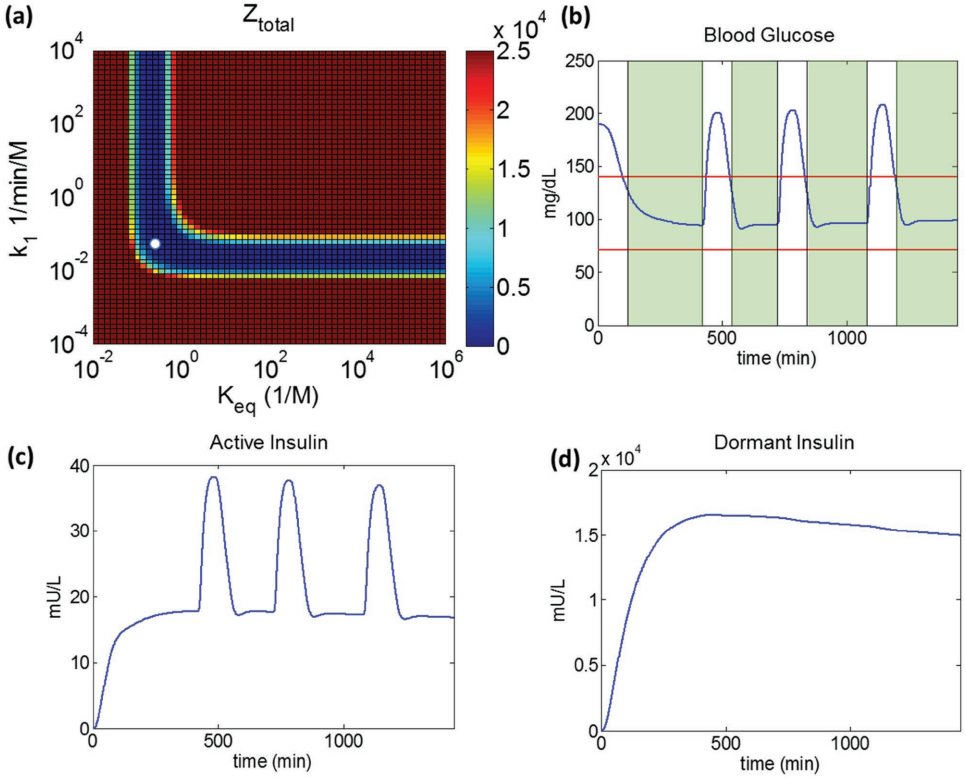

Figure 4. The dynamics for the subcutaneous injection of 3 U kg^{-1} GRI while consuming three meals of 75 g of glucose over the course of a day. a) The contour plot of all blood glucose excursions from the defined criteria (Z_{total}) showing a region of parameter space that can tightly control blood glucose, with a white dot showing the point where $k_1 = 0.07$ M^{-1} min^{-1} and $K_{eq} = 0.33$ M^{-1} that shows good blood glucose control. b) The dynamics of blood glucose throughout the day for the GRI corresponding to the white dot in (a). The red lines show the blood glucose cutoffs of 72 and 140 mg dL^{-1} for evaluating the defined criteria, Z_{total}. The green regions show the regions of integration for evaluating Z_{hi}, which are 120 min after the consumption of a meal or the injection of insulin. The blood glucose remains below the upper the cutoffs within the green region and above the lower cutoff throughout the day. c) The plot showing active blood insulin dynamics for the GRI corresponding to the white dot in (a). d) The plot showing dormant blood insulin dynamics for the GRI corresponding to the white dot in (a).

that as long as the optimal GRI level in the body is maintained, the patient would benefit from proper blood glucose control within the current meal regiment.

3.3. GRI Efficacy

Despite the fact that 3 U kg^{-1} of GRI showed a range of parameters that could effectively control blood glucose, this is significantly higher than the 0.5–1 U kg^{-1}[44] total insulin amounts normally administered daily to Type 1 diabetic patients. In this study, GRI and regular insulin are compared on a mole basis and a unit of GRI is equivalent to a unit of regular insulin despite the differences in pharmacokinetics. Due to the equilibrium between GRI and insulin, the proposed dosing of the GRI is significant. Additionally, current insulin therapies rely on tightly controlled diets to ensure that hypoglycemia or hypoglycemia events are necessarily avoided.[44] To test the effect of GRI dosage, and examine the sensitivity of the meal regiments on optimal GRI parameters, we simulated three different GRI doses (**Figure 5**): 0.5, 3, and 5 U kg^{-1} along with two different meal regiments of (i) three meals consisting of 75 g of glucose given at $t = 420$ min, $t = 720$ min, and $t = 1080$ min, similar to the previous simulations, and (ii) two meals consisting of 75 g of glucose given at $t = 420$ min and $t = 1080$ min, which removes the second meal. Figure 5 shows a limited parameter space so shifts in effective GRI space are more easily observed.

Indeed, when comparing the same insulin dose between different meal plans the range of effective parameters does not change significantly. This is a desired property of overall GRI potency. There are slight differences in the boundaries of the parameter space resulting in safe physiological states. However,

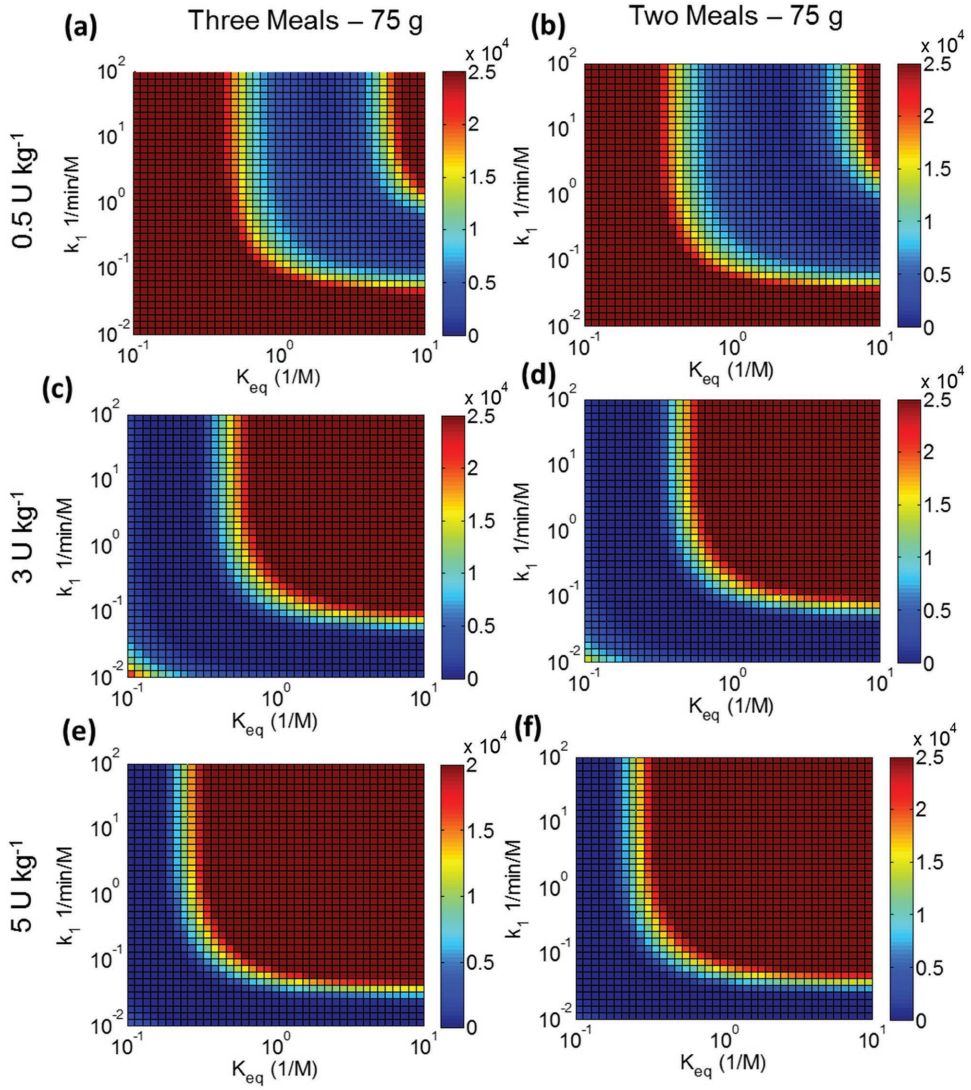

Figure 5. Contour plots showing effective parameter range while altering GRI dosing and meal regiment. a) 0.5 U kg^{-1} of GRI dosed while consuming three meals 75 g. b) 0.5 U kg^{-1} of GRI dosed while consuming two meals 75 g. c) 3 U kg^{-1} of GRI dosed while consuming three meals 75 g. d) 3 U kg^{-1} of GRI dosed while consuming two meals 75 g. e) 5 U kg^{-1} of GRI dosed while consuming three meals 75 g. f) 5 U kg^{-1} of GRI dosed while consuming two meals 75 g.

there is broad overlap between case (i) and case (ii), meaning that a wide range of parameters can be found that produce comparable, optimal glucose control largely independent of the meal regiment. Furthermore, within each meal regiment, the GRI dosage results in a different set of optimal parameters that result in a Z_{total} of zero, with the exception of the 0.5 U kg^{-1} dose, which did not completely force Z_{total} to zero. We assert that this dosing flexibility is particularly advantageous because it suggests that if certain GRI parameters cannot be realized experimentally, then dosing could be altered to optimize control of blood glucose levels, as well allowing customized dosing for each patient. However, care should be taken with the loading of dormant insulin in the blood stream. In the Supplementary Information, we show that for cases where Z_{total} equal to zero, for both 3 and 5 U kg^{-1} doses, ≈29 U of insulin were consumed over the course of the day, which results in insulin consumptions of 13.8% and 8.3%, respectively. The advantage of the higher dose is that blood glucose can be controlled for a longer amount of time, without an additional injection of GRI. However, all GRI formulations inherently carry the risk of the adverse reaction of hypoglycemia from inappropriate insulin release, with a higher dose corresponding to a larger reservoir of dormant insulin circulating within the body.

Dalla Man[32–35] introduced an alternative physiological compartment model trained on clinical data. We compare the results of the Sorensen model above to those using the Dalla Man model in the Supplementary Information. These results highlight that the physiological model employed has a strong effect on the optimal GRI parameter space predicted. However, we note that the two models do present an overlapping space for k_1 and K_{eq} parameters where both yield adequate blood glucose control, supporting the validity of the overall approach outlined in this work.

4. Conclusions

Herein, we present a straightforward approach to designing glucose responsive insulin constructs with increased performance in the human body. Combining pharmacokinetic models of the body with mathematical representations of GRIs, along with desired physiological constraints provide a set of equations amenable to the exploration of efficacious parameter space. The parameter space includes the dissociation constant of glucose, and the corresponding insulin potency, which the medicinal chemist can then incorporate into the molecular design. In this work we considered the case of a freely circulating GRI that can switch from low to high potency states upon binding to glucose in the bloodstream, which was modeled as an equilibrium reaction between glucose and the GRI. This GRI model describes recently reported experimentally engineered insulins specifically designed to interact with glucose in this way.[21] By coupling these equations to a physiological model such as one from Sorensen,[21,26,30] one can explore the parameters affecting GRI design. The modeling reveals that a range of GRI parameters exists within which it is possible to control blood glucose concentration, within prescribed limits, over a 24 h period while consuming three meals of 75 g of glucose with only a single subcutaneous injection of the GRI. Due, to the equilibrium between the dormant and active forms of insulin, changing the amount of GRI dosed will change the range of parameters that result in good blood glucose control. The GRI dosing can be altered in the model until the parameters needed for good glycemic control match experimentally developed GRIs, saving time and experimental iterations for the medicinal chemist. Additionally, our modeling suggests that when certain parameters are used, the GRI functions in such a way that missing a meal during the 24 h period results in stable glucose and insulin levels. In this way, our model provides a basis to assist researchers in optimizing parameters and calculating proper dosing to result in GRIs that provide effective glycemic control and are robust to changes in meal schedule.

Supporting Information

Supporting Information is available from the Wiley Online Library or from the author.

Acknowledgements

This work was supported by the Juvenile Diabetes Research Foundation.

Conflict of Interest

The authors declare no conflict of interest.

Keywords

diabetes, glucose sensing, insulin, pharmacokinetics, smart therapy

Received: May 11, 2017
Revised: June 30, 2017
Published online:

[1] K. G. Alberti, P. Z. Zimmet, *Diabetic Med.* **1998**, *15*, 539.
[2] P. Zimmet, K. G. M. M. Alberti, J. Shaw, *Nature* **2001**, *414*, 782.
[3] P. E. Cryer, S. N. Davis, H. Shamoon, *Diabetes Care* **2003**, *26*, 1902.
[4] J. E. Shaw, R. A. Sicree, P. Z. Zimmet, *Diabetes Res. Clin. Pract.* **2010**, *87*, 4.
[5] D. E. Dewitt, I. B. Hirsch, R. Care, P. Pro, *JAMA* **2003**, *289*, 2254.
[6] O. Veiseh, B. C. Tang, K. a. Whitehead, D. G. Anderson, R. Langer, *Nat. Rev. Drug Discovery* **2015**, *14*, 45.
[7] M. Peyrot, A. H. Barnett, L. F. Meneghini, P. M. Schumm-Draeger, *Diabetic Med.* **2012**, *29*, 682.
[8] R. M. Bergenstal, W. V. Tamborlane, A. Ahmann, J. B. Buse, G. Dailey, S. N. Davis, C. Joyce, T. Peoples, B. A. Perkins, J. B. Welsh, S. M. Willi, M. A. Wood, *N. Engl. J. Med.* **2010**, *363*, 311.
[9] J. C. Pickup, *Nat. Rev. Endocrinol.* **2012**, *8*, 425.
[10] J. C. Pickup, *N. Engl. J. Med.* **2012**, *366*, 1616.
[11] M. J. Webber, D. G. Anderson, *J. Drug Targeting* **2015**, *23*, 651.
[12] K. M. Bratlie, R. L. York, M. A. Invernale, R. Langer, D. G. Anderson, *Adv. Healthcare Mater.* **2012**, *1*, 267.
[13] S. B. Bankar, M. V. Bule, R. S. Singhal, L. Ananthanarayan, *Biotechnol. Adv.* **2009**, *27*, 489.
[14] J. Heller, A. C. Chang, G. Rood, G. M. Grodsky, *J. Controlled Rel.* **1990**, *13*, 295.

[15] G. Albin, T. A. Horbett, B. D. Ratner, *J. Controlled Rel.* **1985**, *2*, 153.
[16] K. Ishihara, M. Kobayashi, N. Ishimaru, I. Shinohara, *Polym. J.* **1984**, *16*, 625.
[17] L. Y. Chu, Y. Li, J. H. Zhu, H. D. Wang, Y. J. Liang, *J. Controlled Rel.* **2004**, *97*, 43.
[18] Z. Gu, T. T. Dang, M. Ma, B. C. Tang, H. Cheng, S. Jiang, *ACS Nano* **2013**, *7*, 6758.
[19] R. Yin, Z. Tong, D. Yang, J. Nie, *Carbohydr. Polym.* **2012**, *89*, 117.
[20] A. Matsumoto, T. Ishii, J. Nishida, H. Matsumoto, K. Kataoka, Y. Miyahara, *Angew. Chem., Int. Ed.* **2012**, *51*, 2124.
[21] D. H.-C. Chou, M. J. Webber, B. C. Tang, A. B. Lin, L. S. Thapa, D. Deng, J. V. Truong, A. B. Cortinas, R. Langer, D. G. Anderson, *Proc. Natl. Acad. Sci. USA* **2015**, *112*, 2401.
[22] Z. Gu, A. A. Aimetti, Q. Wang, T. T. Dang, Y. Zhang, O. Veiseh, H. Cheng, R. S. Langer, D. G. Anderson, *ACS Nano* **2013**, *7*, 4194.
[23] M. Abdekhodaie, X. Wu, *J. Membr. Sci.* **2005**, *254*, 119.
[24] M. J. Abdekhodaie, X. Y. Wu, *J. Membr. Sci.* **2009**, *335*, 21.
[25] G. W. Albin, T. A. Horbett, S. R. Miller, N. L. Ricker, *J. Controlled Rel.* **1987**, *6*, 267.
[26] J. T. Sorensen, *Ph.D. Thesis*, MIT, Cambridge, MA **1985**.
[27] R. S. Parker, F. J. Doyle III, N. a Peppas, *IEEE Trans. Biomed. Eng.* **1999**, *46*, 148.
[28] R. S. Parker, F. J. I. Doyle, J. H. Ward, N. a Peppas, *AIChE J.* **2000**, *46*, 2537.
[29] R. S. Parker, F. J. Doyle III, N. A. Peppas, *Eng. Med. Biol. Mag. IEEE* **2001**, *20*, 65.
[30] G. Bisker, N. M. Iverson, J. Ahn, M. S. Strano, *Adv. Healthcare Mater.* **2015**, *4*, 87.
[31] D. H.-C. Chou, M. J. Webber, B. C. Tang, A. B. Lin, L. S. Thapa, D. Deng, J. V. Truong, A. B. Cortinas, R. Langer, D. G. Anderson, *Proc. Natl. Acad. Sci. USA* **2015**, 1.
[32] C. D. Man, M. Camilleri, C. Cobelli, C. Dalla Man, *IEEE Trans. Biomed. Eng.* **2006**, *53*, 2472.
[33] C. Dalla Man, R. A. Rizza, C. Cobelli, *IEEE Trans. Biomed. Eng.* **2007**, *54*, 1740.
[34] C. D. Man, D. M. Raimondo, R. A. Rizza, C. Cobelli, *J. Diabetes Sci. Technol.* **2007**, *1*, 323.
[35] B. P. Kovatchev, M. Breton, C. Dalla Man, C. Cobelli, *J. Diabetes Sci. Technol.* **2009**, *3*, 44.
[36] P. Hildebrandt, L. Sestoft, S. L. Nielsen, *Diabetes Care* **1983**, *6*, 459.
[37] J. A. Galloway, C. T. Spradlin, R. L. Nelson, S. M. Wentworth, J. A. Davidson, J. L. Swarner, *Diabetes Care* **1981**, *4*, 366.
[38] E. Mosekilde, K. S. Jensen, C. Binder, S. Pramming, B. Thorsteinsson, *J. Pharmacokinet. Biopharm.* **1989**, *17*, 67.
[39] J. Wong, J. G. Chase, C. E. Hann, G. M. Shaw, T. F. Lotz, J. Lin, A. J. Le Compte, *J. Diabetes Sci. Technol.* **2008**, *2*, 658.
[40] J. Wong, J. G. Chase, C. E. Hann, G. M. Shaw, T. F. Lotz, J. Lin, A. J. Le Compte, *J. Diabetes Sci. Technol.* **2008**, *2*, 672.
[41] C. Tarín, E. Teufel, J. Picó, J. Bondia, H. J. Pfleiderer, *IEEE Trans. Biomed. Eng.* **2005**, *52*, 1994.
[42] American Diabetes Association, *Diabetes Care* **2015**, *38*, S8.
[43] E. D. Lehmann, T. Deutsch, *J. Biomed. Eng.* **1992**, *14*, 235.
[44] I. B. Hirsch, *Am. Fam. Physician* **1999**, *60*, 2343.